Spatiotemporal periodic and chaotic patterns in a two-dimensional coupled map lattice system

Fagen Xie [1,2,*] and Gang Hu [1,3]

[1] *China Center of Advanced Science and Technology (World Laboratory), P.O. Box 8730, Beijing 100080, China*

[2] *Institute of Theoretical Physics, Academia Sinica, Beijing 100080, China*

[3] *Department of Physics, Beijing Normal University, Beijing 100875, China*

(Received 18 July 1996)

The pattern dynamics of a two-dimensional coupled map lattice system is studied using both analytical and numerical calculations. Two interesting spatiotemporal periodic patterns are solved analytically. Their stability boundaries for small system size are obtained by linear stability analysis. As the system sizes mismatch the spatial periodicity of the patterns, a frozen random chaotic defect cluster and a slow random propagated chaotic defect string appear. [S1063-651X(96)09712-7]

PACS number(s): 05.45.+b

I. INTRODUCTION

The dynamics of coupled nonlinear systems has attracted great interest in the past decade [1–12]. One such system is the coupled map lattice (CML), which has been demonstrated to be powerful for heuristically understanding the universal features in extended systems in optics, fluids, biology, etc. Rich spatiotemporal complex behaviors, including patterns, domain walls, traveling waves, intermittency, chaos, and developed turbulence, are revealed in the one-dimensional CML [1–9]. An extension of the study of the CML to a two-dimensional lattice was briefly addressed in Ref. [6]. It has been known that the two-dimensional CML system possesses more interesting and complicated spatiotemporal phenomena than the one-dimensional one. A deeper investigation of two-dimensional coupled map systems may be very useful for understanding even more complicated and realistic features of higher-dimensional systems. In this presentation, we focus our attention on the investigation of the two-dimensional CML with a nearest-neighbor coupled interaction in square lattices

$$x_{n+1}(i,j)=(1-\epsilon)f(x_n(i,j))+\frac{\epsilon}{4}[f(x_n(i-1,j)) + f(x_n(i+1,j))+f(x_n(i,j-1)) + f(x_n(i,j+1))], \quad (1)$$

with the periodic boundary conditions $x(i+N_1,j)\equiv x(i,j)$, and $x(i,j+N_2)\equiv x(i,j)$, where N_1 and N_2 are the system sizes in both spatial dimensions. Here n is the discrete time index, $i(=0,1,2,\ldots,N_1-1)$ and $j(=0,1,2,\ldots,N_2-1)$ are the spatial indices in the horizontal and vertical directions, respectively, and ϵ is the diffusive coupling strength. The local mapping function $f(x)$ is chosen to be the logistic map $f(x)=ax(1-x)$, with a the nonlinear parameter. In Ref. [6], Kaneko numerically discovered a few interesting phenomena such as pattern selection and chaotic string in the system (1). However, more detailed analytical discussions have not been provided. In Sec. II, we derive some interesting periodic patterns of the system. Their stability boundaries for small system size in the parameter plane are also worked out analytically. In Sec. III, we investigate the dependence of the spatiotemporal patterns on the system size. As the system size mismatches the spatial periodicity of these patterns, two surprising and interesting phenomena, such as a frozen random chaotic defect cluster and a slow, randomly propagated chaotic defect string (i.e., the chaotic defect string keeps moving and wanders in the two-dimensional space like a Brownian particle), are found. Finally, we give some conclusions in Sec. IV.

II. SPATIOTEMPORAL PERIODIC PATTERNS IN A TWO-DIMENSIONAL CML

In a one-dimensional nearest-neighbor coupling CML, many of spatiotemporal periodic patterns have been obtained by analytical and numerical methods due to the high symmetry [8]. In this section we discuss some periodic patterns in the two-dimensional CML. We will denote the temporal period m as T_m, spatial period n as S_n. It is natural to first study patterns with small-time and -space periods. The simplest one is $T_2S_{i2}S_{j2}$ state, which has period 2 for both time and two spatial directions. The spatial structure of this state is schematically shown in Fig. 1(a). Here x_1 and x_2 satisfy

$$x_2=(1-\epsilon)f(x_1)+\epsilon f(x_2),$$

$$x_1=(1-\epsilon)f(x_2)+\epsilon f(x_2), \quad (2)$$

which can be solved as

*Electronic address: xiefg@itp.ac.cn

$$x_{1,2}=\frac{1+a-2a\epsilon\pm\sqrt{(1+a-2a\epsilon)^2-4(1-a)(1-\epsilon)-8a(1-\epsilon)^2}}{2a(1-2\epsilon)}, \tag{3}$$

which is a period-2 wave pattern running in both spatial directions. Although the solutions have the same form as in the one-dimensional CML (see Ref. [8]), the eigenvalues are different. The stability condition for this state at $N_1=2,N_2=2$ is determined by the largest eigenvalue among all the eigenvalues of the 4×4 linear stability matrix

$$J=\begin{pmatrix} (1-\epsilon)f_1 & \frac{\epsilon}{2}f_2 & \frac{\epsilon}{2}f_2 & 0 \\ \frac{\epsilon}{2}f_1 & (1-\epsilon)f_2 & 0 & \frac{\epsilon}{2}f_1 \\ \frac{\epsilon}{2}f_1 & 0 & (1-\epsilon)f_2 & \frac{\epsilon}{2}f_1 \\ 0 & \frac{\epsilon}{2}f_2 & \frac{\epsilon}{2}f_2 & (1-\epsilon)f_1 \end{pmatrix}\begin{pmatrix} (1-\epsilon)f_2 & \frac{\epsilon}{2}f_1 & \frac{\epsilon}{2}f_1 & 0 \\ \frac{\epsilon}{2}f_2 & (1-\epsilon)f_1 & 0 & \frac{\epsilon}{2}f_2 \\ \frac{\epsilon}{2}f_2 & 0 & (1-\epsilon)f_1 & \frac{\epsilon}{2}f_2 \\ 0 & \frac{\epsilon}{2}f_1 & \frac{\epsilon}{2}f_1 & (1-\epsilon)f_2 \end{pmatrix},$$

where $f_{1,2}=a(1-2x_{1,2})$. The matrix J can be put into a block-diagonal form by a unitary transformation as

$$J'=\begin{pmatrix} (1-\epsilon)^2f_1f_2 & 0 & 0 & 0 \\ 0 & (1-\epsilon)^2f_1f_2 & 0 & 0 \\ 0 & 0 & (1-\epsilon)^2f_1f_2+\epsilon^2f_2^2 & \epsilon(1-\epsilon)f_1(f_1+f_2) \\ 0 & 0 & \epsilon(1-\epsilon)f_2(f_1+f_2) & (1-\epsilon)^2f_1f_2+\epsilon^2f_1^2 \end{pmatrix}.$$

Thus the corresponding eigenvalues are

$$\lambda_{1,2}=(1-\epsilon)^2f_1f_2,$$

$$\lambda_{3,4}=\frac{2(1-\epsilon)^2f_1f_2+\epsilon^2(f_1^2+f_2^2)\pm\sqrt{[2(1-\epsilon)^2f_1f_2+\epsilon^2(f_1^2+f_2^2)]^2-4(1-2\epsilon)^2f_1^2f_2^2}}{2}. \tag{4}$$

The stability boundaries determined by these critical eigenvalues are shown in Fig. 2 by the solid lines.

Another interesting state $T_2S_{i4}S_{j2}$ or $T_2S_{i2}S_{j4}$ can be easily deduced from the $T_2S_{i2}S_{j2}$ state. The spatial structure of the state is schematically shown in Fig. 1(b) or 1(c). Here x_1 and x_2 are also given by Eqs. (2) and (3), except ϵ should be replaced by $\frac{3}{4}\epsilon$. Thus, if there exists a $T_2S_{i2}S_{j2}$ state at ϵ_0, then there must be a $T_2S_{i4}S_{j2}$ or a $T_2S_{i2}S_{j4}$ state at $\frac{4}{3}\epsilon_0$ and, of course, the system size must match the spatial periodicity of the pattern. With some simple algebra calculations, the critical values of the stable $T_2S_{i4}S_{j2}$ or $T_2S_{i2}S_{j4}$ state are just $\frac{4}{3}$ times that for the $T_2S_{i2}S_{j2}$ state. The stability boundaries of the state are shown in Fig. 2 by dashed lines for $N_1=4,N_2=2$, or $N_1=2,N_2=4$.

As the system size becomes large and the symmetry of the system becomes very high, the number of attractors increases rapidly due to the high symmetry. Therefore, an interesting and significant problem naturally arises whether these periodic states for the small system size still exist and are stable as the system size increases. As long as the system size matches their spatial periodicity, these patterns always exist in the same parameter region (that is obvious). However, enlarging the phase space may result in some changes of their stability boundaries. Moreover, the transient process for reaching these patterns may become very long. The stability analysis of these patterns for large system size has been formally and briefly discussed in Ref. [8]. Here we simply investigate the problem by numerical computation. Figure 3 shows several snapshots of an evolution process of the system for $N_1=N_2=50$, $a=4$, and $\epsilon=0.15$, where the $T_2S_{i2}S_{j2}$ state is stable. We choose the random initial conditions in (0,1) throughout the paper. At the first time stage, the behavior of the system is random motion and few sites arrive at the periodic state forming small $T_2S_{i2}S_{j2}$ clusters [see Fig.

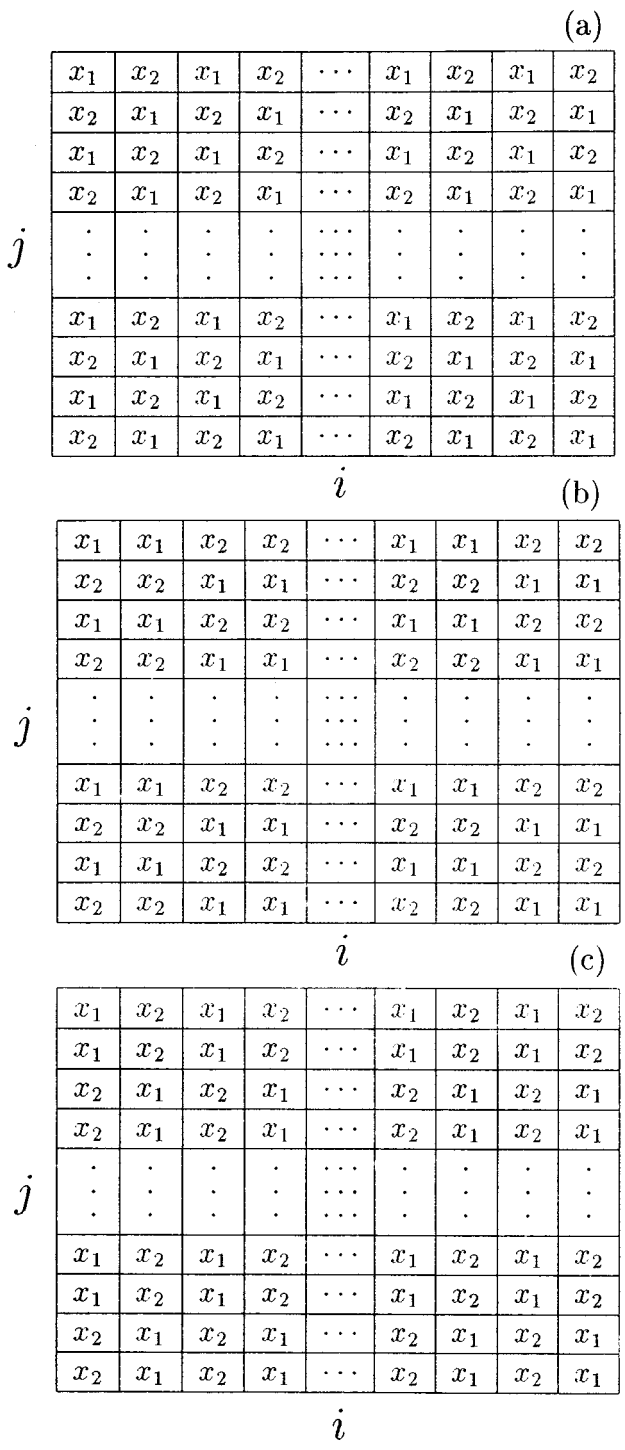

FIG. 1. Schematic spatiotemporal periodic patterns (a) $T_2S_{i2}S_{j2}$, (b) $T_2S_{i4}S_{j2}$, and (c) $T_2S_{i2}S_{j4}$.

3(a)]. After a transient process (309 iterations), half of the remaining lattices arrive at this period-2 state [see Fig. 3(b)]. Figure 3(c) is the final spatiotemporal period-2 pattern after 12 498 iterations (it was reported as a checkerboard pattern in Ref. [6]). Several snapshots for another interesting evolution process are shown in Fig. 4 for $N_1=N_2=52$, $a=4$, and $\epsilon=0.2$. From Fig. 4, it is clear that the system finally settles down into the $T_2S_{i2}S_{j4}$ pattern after a very complicated and longer transient process (after 53 134 iterations).

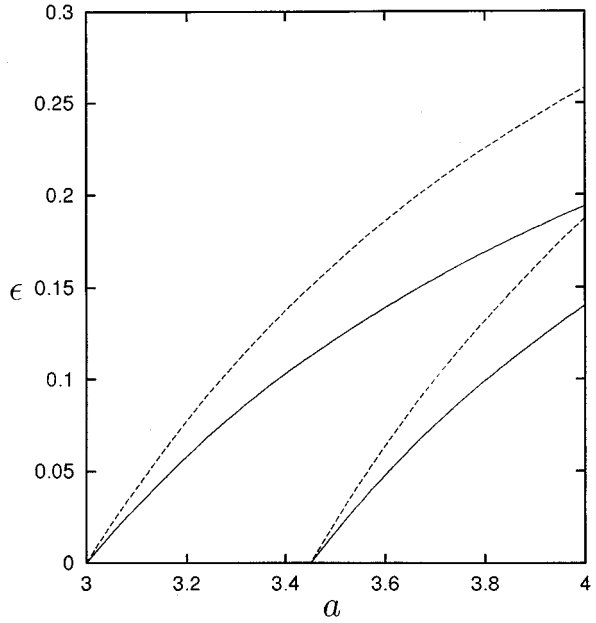

FIG. 2. Stability boundaries for $T_2S_{i2}S_{j2}$ ($N_1=N_2=2$, solid lines), $T_2S_{i4}S_{j2}$ ($N_1=4,N_2=2$, dashed lines), or $T_2S_{i2}S_{j4}$ ($N_1=2$, $N_2=4$).

III. FROZEN RANDOM CHAOTIC DEFECT CLUSTER AND SLOW RANDOM PROPAGATED CHAOTIC DEFECT STRING IN A TWO-DIMENSIONAL CML

In the preceding section, we discussed the pattern dynamics for even system size, which matches the spatial periodicity of the given states. What happens when the system size mismatches their spatial periodicity [i.e., N_1 or N_2 (or both) is (are) taken as odd]? In the following, we investigate the interesting problem for the $T_2S_{i2}S_{j2}$ pattern only.

First, we let the size of one spatial direction take an odd number and the other remains even. For instance, we take all parameters to be the same as those in Fig. 3, except we replace $N_2=50$ by 51. Now the $T_2S_{i2}S_{j2}$ pattern cannot be stable due to the mismatch of the odd size number of the j direction. We show several snapshots of an evolution process in Fig. 5. From the figure, a very interesting and surprising phenomenon, a parallel chaotic defect cluster (the width is near eight sites, the other sites stay at the period-2 state), appears after some transient iterations. As long as the chaotic defect cluster is formed along the i direction, it is frozen forever (forever in the sense that the time period for the frozen pattern numerically tested is already incomparably larger than the transient time).

Comparing Fig. 5(c) with Fig. 5(b), the pattern is almost the same, although the system evolves another 10^5 iterations. The frozen feature can be more clearly observed in Fig. 6. We plot the time $T_{i,j}$ against i,j, where $T_{i,j}$ is the first time for the (i,j)th site to be excited from the period-2 state, starting from Fig. 5(c). The times for these sites, which do not belong to the chaotic defect pattern, are almost infinity (the white region in Fig. 6). Therefore, the frozen character is clear. Furthermore, the position of the frozen pattern strongly

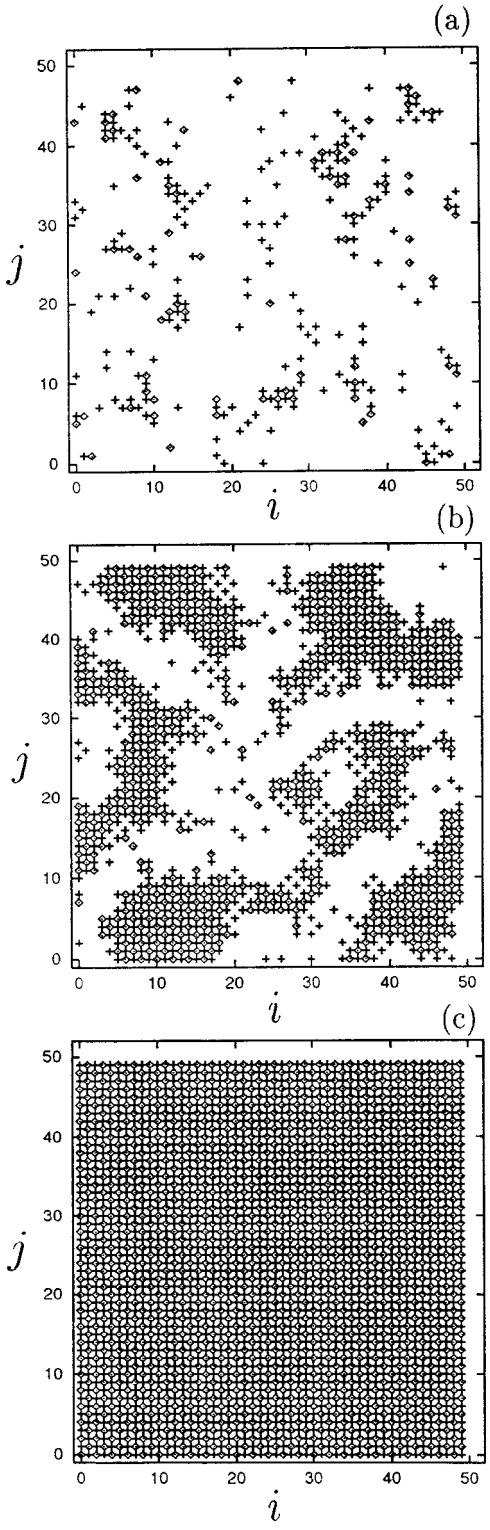

FIG. 3. Snapshots of an evolution process for $a=4$, $\epsilon=0.15$, and $N_1=N_2=50$. The diamonds and pluses show that the sites reach the values of $x_1\pm10^{-3}$ and $x_2\pm10^{-3}$, respectively, where x_1,x_2 is the period-2 state in Eq. (3). (a) $n=60$, (b) $n=309$, and (c) $n=12\,498$.

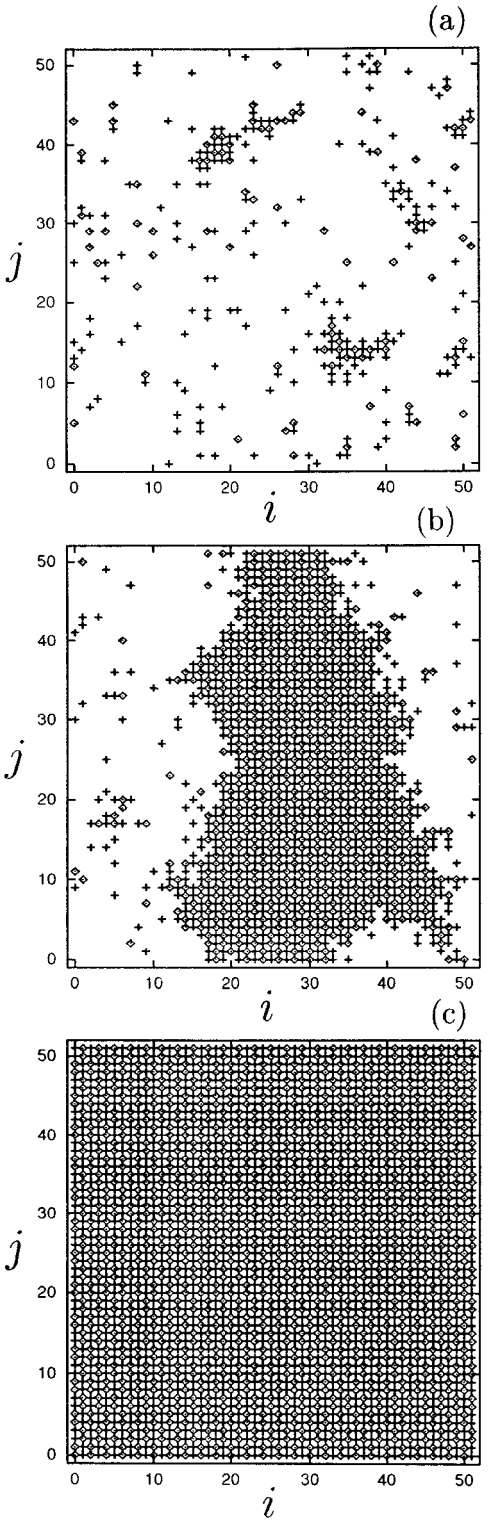

FIG. 4. Same as in Fig. 3, but for $a=4$, $\epsilon=0.2$, and $N_1=N_2=52$. (a) $n=12\,624$, (b) $n=42\,250$, and (c) $n=53\,134$.

depends on the random initial conditions chosen. In order to understand the frozen feature, we plot the evolutions of the sites with $i=N_1/2$ (the characteristics for other i values are the same) in Fig. 7. Some features are worth mentioning. For the sites in the center of the frozen chaotic defect cluster, the dynamical behavior is two-large-band chaotic motion. But the widths of the chaotic bands damp exponentially as the site distance in the j direction from the center of the frozen chaotic defect cluster increases [see Fig. 7(c)]. An empirical formula

$$|x(i,j_c\pm m)-\hat{x}|\leqslant|\mathbf{A}|e^{-\beta m} \tag{5}$$

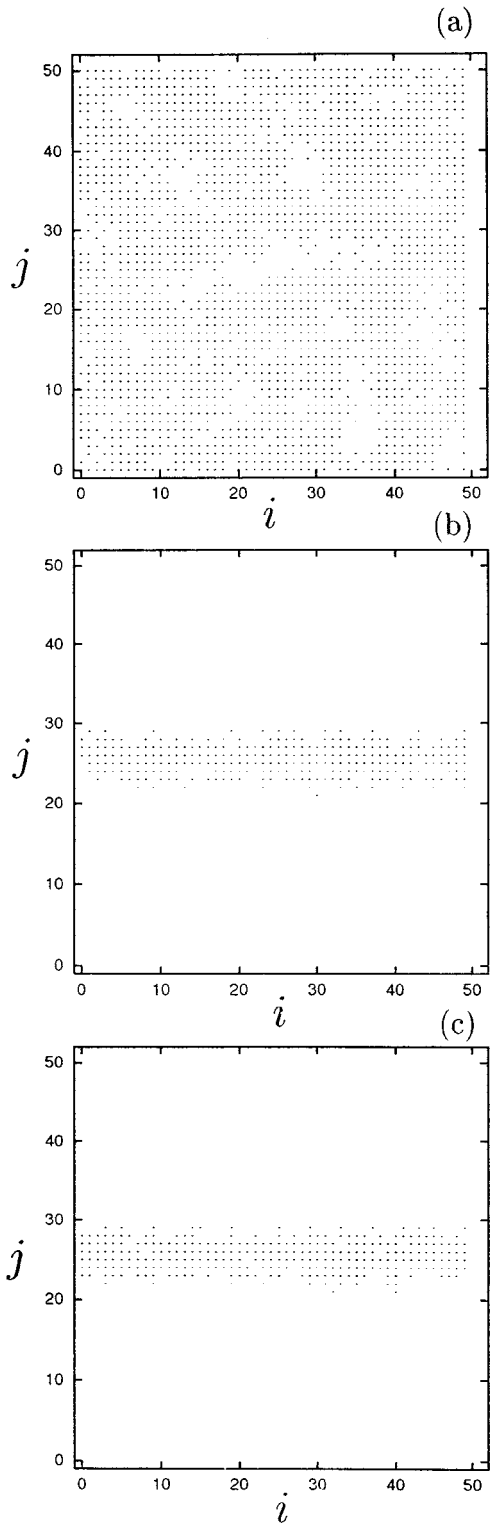

FIG. 5. Same as in Fig. 3, but for $a=4$, $\epsilon=0.15$, $N_1=50$, and $N_2=51$. If $|x_n(i,j)-\hat{x}|>10^{-3}$ [$\hat{x}$ is the period-2 state in Eq. (3)], the corresponding pixel is black; otherwise it stays white. (a) $n=100$, (b) $n=100\,100$, and (c) $n=200\,100$. A parallel frozen chaotic defect cluster is clearly observed in (b) and (c).

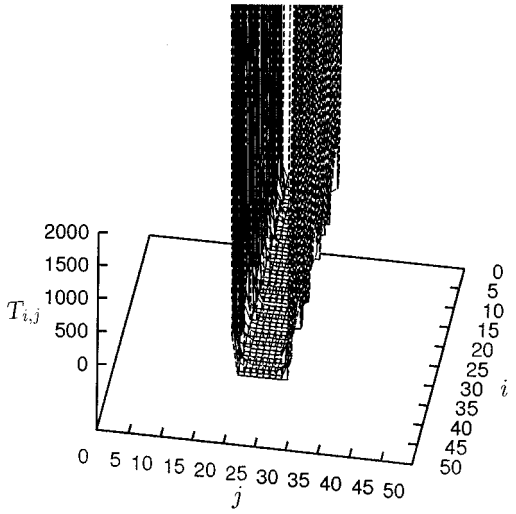

FIG. 6. $T_{i,j}$ plotted against i,j. $T_{i,j}$ is the iteration number for the (i,j)th site to be excited for the first time, starting from Fig. 5(c). A site is regarded as excited as $|x_n(i,j)-\hat{x}|>10^{-3}$, where $\hat{x}$ is the same as in Fig. 5.

fits well the actual widths of the chaotic bands in Fig. 7(c) for an arbitrary i value. In Eq. (5), j_c denotes the center site in the frozen chaotic defect cluster and $\hat{x}=(x_1,x_2)$ is the period-2 state in Eq. (3). The envelopes of the bands shown in Fig. 7(c) are time independent. After some transient iterations, the envelopes are asymptotically approached and frozen forever. The amplitude of $\mathbf{A}=(A_1,A_2)$ depends on the control parameters a and ϵ. The exponent β can be calculated exactly. The main points for the computation are the following. First, as $|j-j_c|$ is large, linearization of the derivations from the period-2 state can be valid. In the linear case the margin certainly maps to the margin itself. Therefore, the margin is a stationary period-4 state of the system. Inserting Eq. (5) into the linearized Eq. (1), we immediately obtain

$$a(1-\epsilon)(1-2x_1)A_1-\left[a\epsilon(1-2x_2)\frac{\sinh\beta}{2}+1\right]A_2=0,$$

$$\left[a\epsilon(1-2x_1)\frac{\sinh\beta}{2}+1\right]A_1+a(1-\epsilon)(1-2x_2)A_2=0, \tag{6}$$

leading to the condition

$$\begin{vmatrix} a(1-\epsilon)(1-2x_1) & -\left[a\epsilon(1-2x_2)\frac{\sinh\beta}{2}+1\right] \\ \left[a\epsilon(1-2x_1)\frac{\sinh\beta}{2}+1\right] & a(1-\epsilon)(1-2x_2) \end{vmatrix}=0, \tag{7}$$

from which β can be given analytically. At $a=4$, $\epsilon=0.15$, we have $x_1=0.458\,414$ and $x_2=0.898\,729$, and then get $\beta\approx 0.92$, which is confirmed by numerical simulations.

If both N_1 and N_2 are taken as odd, the behavior of the system is dramatically changed. The frozen chaotic defect cluster is now replaced by a slow, randomly propagated chaotic defect string (i.e., the chaotic defect string keeps moving and wanders in space like a Brownian particle). With parameters the same as those in Fig. 5, except for $N_1=51$, we plot

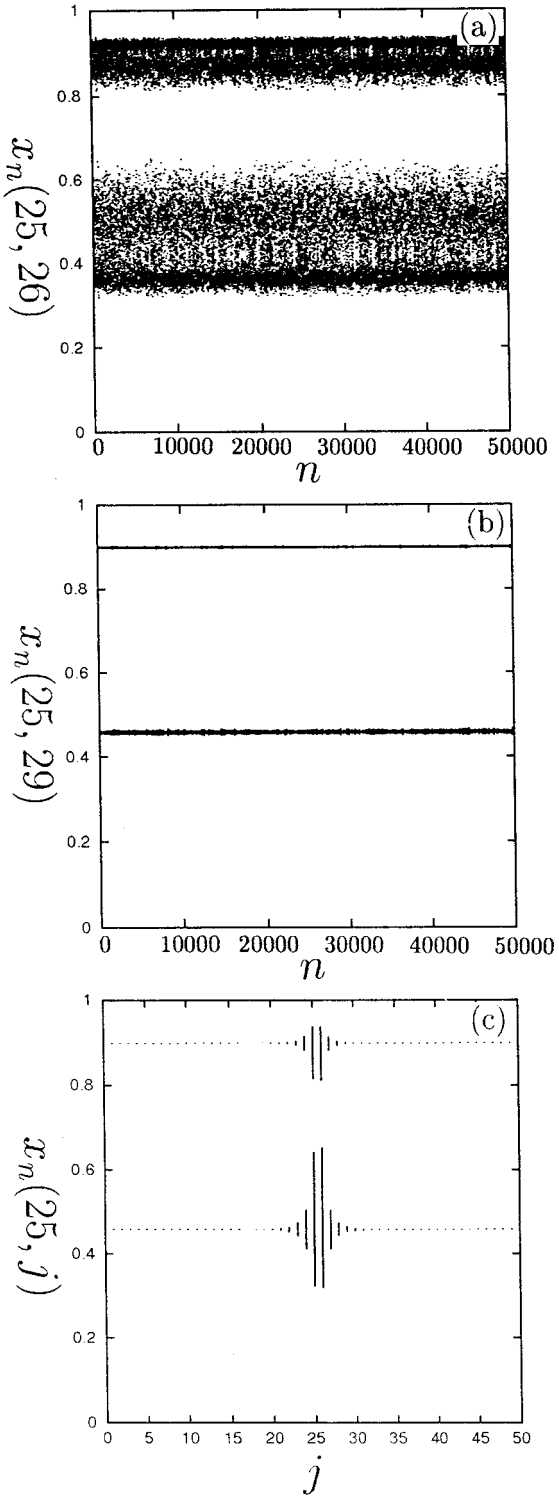

FIG. 7. (a) $x_n(25,26)$ plotted vs n with the same parameters as in Fig. 5. The motion is two-large-band chaos. (b) $x_n(25,29)$ plotted vs n. In comparison with (a), the two bandwidths are much smaller. (c) $x_n(25,j)$ plotted vs j in 2500 iterations after the transient process. The envelopes are frozen.

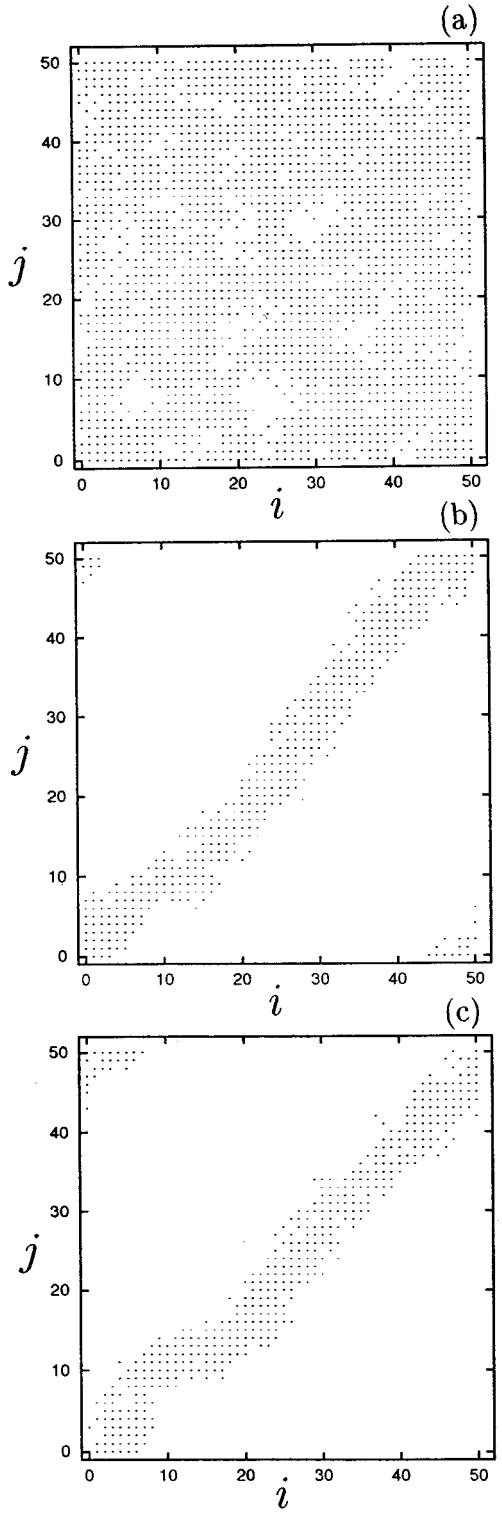

FIG. 8. Same as in Fig. 5 for the same parameters, except $N1=51$. (a) $n=100$, (b) $n=100\ 100$, and (c) $n=200\ 100$. A slow propagation of chaotic defect string from (b) to (c) can be observed.

a spatiotemporal process in Fig. 8 in the same manner as in Fig. 5. After the transient iterations, a near linear chaotic defect cluster (the width is also near eight sites) is organized [see Fig. 8(b)]. The magnitude of the slope of the chaotic defect string is near $N2/N1\approx 1$ (the magnitude of the slope remains $N2/N1$ when $N_1\neq N_2$). This chaotic defect string randomly propagates slowly along the vertical direction of the chaotic defect string through the coupling interaction [see Fig. 8(c)]. The slow randomly propagation feature is shown in Fig. 9, which is plotted in the same manner as in Fig. 6. It

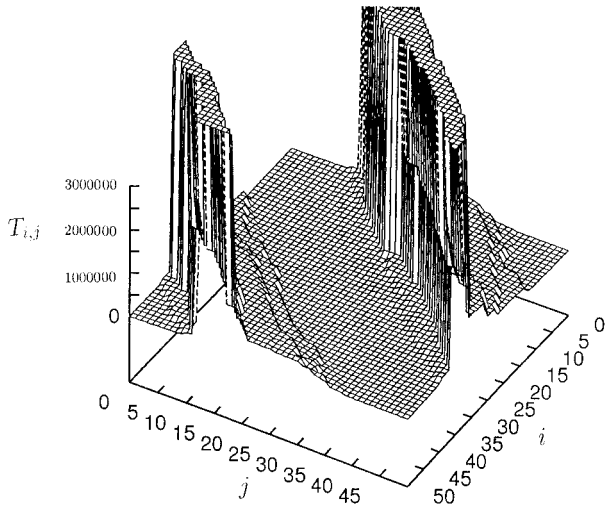

FIG. 9. Same as in Fig. 6, but for the same parameters as in Fig. 8 [starting from Fig. 8(c)]. The slow propagation property is clear.

takes a very long time for the lattice sites far from those in the chaotic defect string to be excited from the period-2 pattern. The cause of the slow random propagation is that the exponential decay law of Eq. (5) for Fig. 7 is now broken. The motion of every site in the chaotic defect string can arrive at the whole (0,1) phase space. We also plot the time evolutions for some sites in Fig. 10 at the same parameters as in Fig. 8. The dynamics exhibits a very interesting phenomenon, a characteristic of on-off intermittency [13–15]. Each site stays near the ''off'' state (defined as the period-2 state in Sec. II) for a long time and suddenly departs from, and then returns again quickly to, the ''off'' state. In Fig. 10(c) we present the laminar phase distribution of Fig. 10(a), showing a nearly $-\frac{3}{2}$ power-law decay scaling.

IV. CONCLUDING REMARKS

In conclusion, we have studied both analytically and numerically the interesting pattern dynamics in a two-dimensional CML system. First, two types of spatiotemporal periodic patterns are solved analytically, based on the symmetric property of the CML system. Their stability boundaries for small system size are obtained by a linear stability analysis. Enlarging the phase space results in a very long and complicated transient process before the system falls in these spatiotemporal patterns when the system size matches their spatial periodicity.

Second, as the system size mismatches the spatial periodicity of the $T_2S_{i2}S_{j2}$ pattern, two surprising and interesting chaotic patterns appear at the same parameter values. If the size of only one spatial direction (odd) mismatches the pattern, a frozen random chaotic defect cluster is formed after some transient iterations. The amplitudes of the chaotic motions damp exponentially as the distance of the site measured from the site at the center of the chaotic defect cluster increases. However, as the sizes of both spatial directions are odd, a slow, randomly propagated chaotic defect string appears. The exponential decay law is broken. The motion of

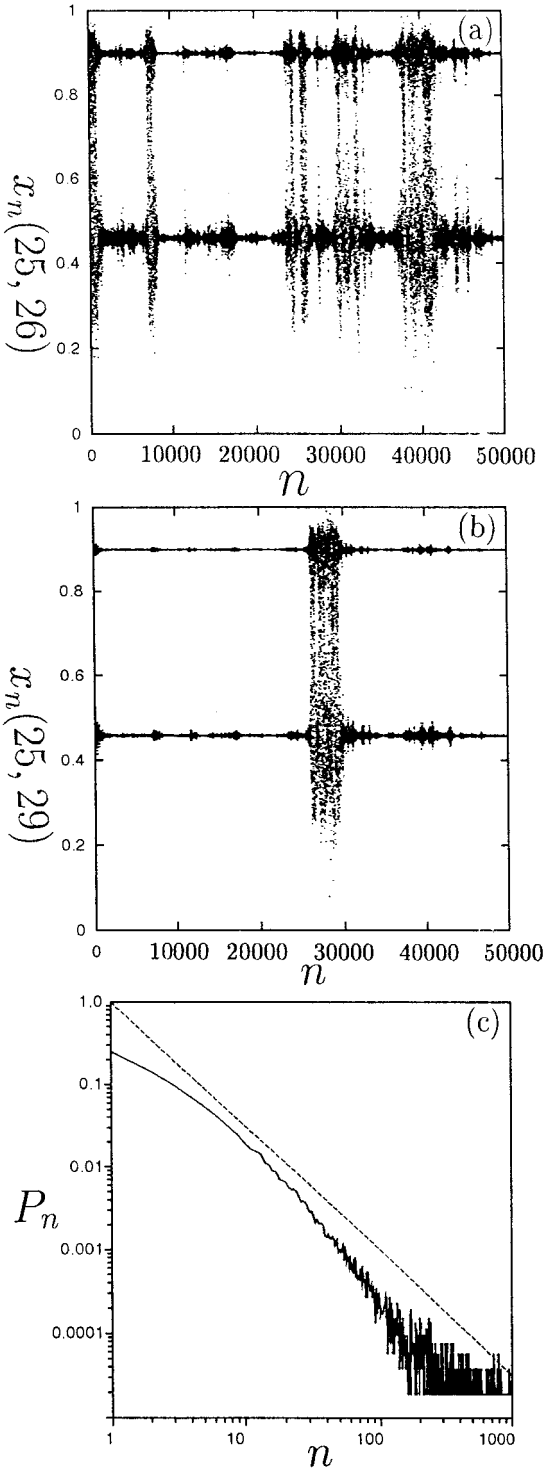

FIG. 10. (a) $x_n(25,26)$ plotted vs n with the same parameters as in Fig. 8. (b) $x_n(25,29)$ plotted vs n. The chaotic motion visits the whole (0,1) phase space. The feature of on-off intermittency is clear. (c) The laminar phase distribution of (a), showing nearly a $-\frac{3}{2}$ power-law decay scaling (the dashed line).

each site extends to the whole (0,1) phase space. The time behavior for every site displays an interesting on-off intermittency. These defects can be regarded as topological defects, of which the features depend on the spatial dimension of the system.

[1] K. Kaneko, Prog. Theor. Phys. **72**, 480 (1984); **74**, 1033 (1985).
[2] K. Kaneko, Physica D **23**, 436 (1986); **34**, 1 (1989).
[3] J. P. Crutchfield and K. Kaneko, in *Directions in Chaos*, edited by Hao Bailin (World Scientific, Singapore, 1987), p. 272.
[4] J. P. Crutchfield and K. Kaneko, Phys. Rev. Lett. **60**, 2715 (1988).
[5] K. Kaneko, Phys. Lett. A **125**, 25 (1987); **149**, 105 (1990).
[6] K. Kaneko, Physica D **37**, 60 (1989).
[7] P. M. Gade and R. E. Amritkar, Phys. Rev. E **47**, 143 (1993).
[8] Zhilin Qu and Gang Hu, Phys. Rev. E **49**, 1099 (1994); **50**, 163 (1994).
[9] F. H. Willeboordse and K. Kaneko, Phys. Rev. Lett. **73**, 533 (1994); Physica D **85**, 428 (1995).
[10] K. Wiesenfeld and P. Hadley, Phys. Rev. Lett. **62**, 1335 (1989).
[11] D. Domínguez and H. A. Cerdeira, Phys. Rev. Lett. **71**, 3359 (1993); Phys. Rev. B **52**, 513 (1995).
[12] H. G. Winful and L. Rahman, Phys. Rev. Lett. **65**, 1575 (1990).
[13] N. Platt, E. A. Spiegel, and C. Tresser, Phys. Rev. Lett. **70**, 279 (1993).
[14] J. F. Heagy, N. Platt, and S. M. Hammel, Phys. Rev. E **49**, 1140 (1994).
[15] Fagen Xie, Gang Hu, and Zhilin Qu, Phys. Rev. E **52**, R1265 (1995).